

Cortical blood flow through individual capillaries in rat vibrissa S1 cortex: Stimulus induced changes in flow are comparable to the underlying fluctuations in flow.

David Kleinfeld

Department of Physics and Graduate Program in Neurosciences, University of California, La Jolla, California USA.

Abstract

Cortical blood flow was probed via the motion of red blood cells (RBCs) in individual capillaries that lay as much as 600 μm below the pia matter of primary somatosensory cortex in rat. The flow was quite variable, with a speed of 0.8 ± 0.5 mm/s (mean \pm SD) and a flux of 60 ± 40 RBC/s, averaged over all capillaries and over time. The fluctuations in the flow were dominated by a spectral band near 0.1 Hz. This band coincides with the spectral band of fluctuations previously seen across whole capillary beds with optical (*Mayhew, Askew, Zeng, Porrill, Westby, Redgrave, Rector and Harper. 1996. Neuroimage 4:183*) and fMRI (*Mitra, Ogawa, Hu and Ugurbil. 1997. Mag. Reson. Med. 37:511*) imaging techniques.

Time-locked increases in the flow of RBCs within individual capillaries were observed in response to stimulation of multiple vibrissae at natural levels of deflection. The magnitude of the stimulus evoked change in speed was, at most, equal to 20 % of the basal speed. This change is comparable to the level of the fluctuations in speed seen in single capillaries. Thus, changes in flow evoked by natural stimuli are largely masked by basal fluctuations.

In toto, the results of our study suggest that fluctuations at the level of the microvasculature limit the sensitivity of brain imaging techniques, at least at low frequencies.

Correspondence:

David Kleinfeld

Department of Physics 0319

University of California, San Diego

9500 Gilman Drive

La Jolla, CA 92093

dk@physics.ucsd.edu

FAX: 858-534-7697

Voice: 858-822-0342

Brain homeostasis depends on adequate levels of blood flow to insure the delivery of nutrients and to facilitate the removal of metabolites and heat. The exchange of material between constituents in the blood and neurons and glia occurs at the level of individual capillaries. Further, sensory stimulation, or even ideation, may lead to an increase in the electrical activity within populations of neurons that subsequently results in a shift in blood flow between activated and quiescent regions [1]. These shifts are of sufficient duration and magnitude to form the basis of imaging techniques in which neuronal activity is inferred from changes in blood flow and blood oxygenation [2;3]. However, such changes are only observed with extensive averaging over time and/or trials.

What is the noise source that limits the sensitivity of brain imaging techniques? An elegant anatomical study performed by Morri et. al [4] provides graphic illustration that the capillary bed is tortuous, with a high degree of connectivity in the form of “T”-junctions and closed loops that bridge between arterioles and venules (Fig. 1). Other studies provide evidence for local sphincters in the arterioles, which suggests that blood flow is controlled at the level of only a few capillaries [5]. In light of analogies between the geometry of the microvasculature and that of models for transport in weakly connected networks [6], one may conjecture that the basal flow through capillaries may support a multitude of stable flow patterns. Further, the flow may be highly variable if small changes in the microvasculature result in a shift among such patterns. The present physiological relevance of such variability is that it may set a baseline level for meaningful changes in blood flow that occur as a result of changes in brain electrical activity and/or metabolism.

Here we address the issue of determining the magnitude of the basal fluctuations in red blood cell (RBC) flow in individual capillaries in comparison with the change in flow in response to natural stimuli. We used two-photon laser scanning microscopy as a means to study flow deep to the pia matter with diffraction limited optical resolution [7;8]. Flow was imaged at depths up to 600 μm [9], which corresponds to

the level of layer 4. This layer is the primary locus of afferent input and, consistent with a large density of presynaptic terminals and their concomitant metabolic needs, contains the highest density of vasculature throughout the neocortex [10].

Adult Sprague-Dawley rats that were anesthetized with urethane served as our preparation. We report on results for 8 animals and 42 capillaries.. Contrast was supplied by labeling the blood serum with fluorescein isothiocyanate-dextran (77 kD) in physiological saline; the concentration of dye in the serum was estimated to be 300 μ M. The RBCs appeared as dark objects on a fluorescent background [11]. Natural stimulation was performed by tapping a group of approximately 15 vibrissae that encompassed the straddlers and rostral vibrissae of rows B through E. Sinusoidal motion, typically 2° in amplitude, was delivered at 10 Hz for a period of 1 s, in concurrence with the rate at which rats palpate objects with their vibrissae [12]. The extent of cortical activation by the stimulus was inferred from an electrocorticogram (ECoG).

We readily imaged single microvessels and the surrounding vasculature at submicron resolution (Figs. 2a and b). Successive, rapidly acquired planar images of such microvessels revealed a train of dark objects that moved across a sea of fluorescently labeled serum (Fig. 2c). The dark spots are red blood cells. The change in position of the spots between successive images is proportional to the speed (arrows; Fig. 2c).

In general, we had insufficient temporal resolution to characterize the motion of RBCs from planar images of the entire vessel. Thus we acquired repetitive line scans along the central axis of a capillary. The data comprise a matrix with one spatial, x , and one temporal, t , dimension. In this mode, the motion of RBCs leads to dark bands in the data set (Fig. 2d). The average time between bands at a fixed position, denoted Δt , is inversely proportional to the *flux*, the average distance between bands at a fixed time, denoted Δx , is inversely proportional to the *linear density* of RBCs, and the average

slope of the band, $\Delta t/\Delta x$, is inversely proportional to the *speed* of the RBCs (Fig. 2c). These three quantities are related by $flux = linear\ density \cdot speed$. The average flux of RBCs was determined by manually counting the number of bands in successive, 0.5 s intervals. The average speed of RBCs in either 0.05 or 0.1 s intervals was determined by an automatic procedure.

The passage of RBCs appeared to occur at irregular intervals (Figs. 3a-c). The spectral composition of this variability was not uniform; in essentially all cases the speed exhibited a spectral peak between 0.1 and 0.2 Hz (Fig. 3d). The time-averaged properties of the blood flow through each vessel were examined in terms of the values of the speed and flux averaged over a 20 s interval. We observed that the speed and flux vary over a range of values mainly between 0 and 1 mm/s, and 0 and 100 RBC/s, respectively, and that they linearly track each other at low values of flux (Fig. 3e). At high values of flux the speed has a tendency to plateau (Fig. 3e).

We observed frequent instances of highly irregular flow in which the speed and flux changed suddenly (Fig. 3f) or in which individual RBCs stalled for extended periods of time (Fig. 3g). The most extensive irregularities occurred at the confluence of 3 vessels that formed a “T” junction. We simultaneously scanned the two collinear arms and often observed stalls in one arm, as well as sustained reversals in the direction of flow in one or both arms (Fig. 3h).

To examine the effect of stimulation on the flux and linear density of the RBCs, as well as explore the issue of single-trial variability, we consider the analysis of records that were free of stalls or other large irregularities over an entire 128 s period of acquisition. For the example of Fig. 4a, we observed considerable trial-to-trial variability in the value of the stimulus-induced change in the speed of RBCs (top line; Fig. 4a), as well as in the change in flux (second line). An examination of the averaged quantities for this trial reveals that the flux as well as the speed transiently increase upon stimulation (Fig. 4b). Nonetheless, the spectral composition of the

speed indicates that the magnitude of the peak at the repetition rate of the stimulus (0.05 Hz; ◆ in Fig. 4c) is similar to the magnitude for peak that corresponds to low frequency oscillations (0.1 Hz; ★ in Fig. 4c.). The latter peak is present independent of stimulation (Fig. 4c).

A final point concerns the possibility that the capillary flow was largely unresponsive to stimulation in our preparations. As a control experiment, we measured the change in flow of RBCs in response to mild electrical shock to the tail. We collected data from both vibrissa S1 cortex as well as more medial parts of S1 cortex, which respond to stimulation of the trunk and lower limbs. In all cases we observed changes in flow that were 50 to 100 % of the basal level, as typified by the data of figure 5 and consistent with past work using electrical stimulation [13]. This implies that the level of response we observe with natural vibrissa stimulation is not an artifact of compromised physiology.

To summarize, we observe low frequency fluctuations in the speed of RBC flow. The frequency of these oscillations are similar to those reported for the speed of RBCs imaged in capillaries close to at the cortical surface by wide-field techniques [14] and inferred from laser-Doppler measurements [15]. Further, oscillations with a similar spectral character are observed with intrinsic optical imaging of cortical function in rat [16] and result in changes in blood flow that are coherent over distances of 1 mm or more across cortex [17]. These oscillations are generally termed “vasomotion” and, consistent with their extended correlations, are believed to result from oscillations in the arterial supply [18;19]. From the perspective of functional imaging of nervous activity, these oscillations appear as a physiological noise source that are likely to limit the sensitivity of optical or magnetic resonance imaging techniques [16;20] in which the contrast mechanism is related to changes in blood flow [21].

Acknowledgement: I thank my past and present collaborators, Winfried Denk, Fritjof Helmchen, Partha P. Mitra, Nozomi Nishimuri, and Philbert S. Tsai, for their efforts. Work sponsored by the NINDS.

1. Woolsey, T. A., Rovainen, C. M., Cox, S. B., Henger, M. H., Liange, G. E., Liu, D., Moskalenko, Y. E., Sui, J., and Wei, L., Neuronal units linked to microvascular modules in cerebral cortex: Response elements for imaging the brain. *Cerebral Cortex*, 1996. **6**: p. 647-660.
2. Raichle, M. E., Circulatory and metabolic correlates of brain function in normal humans, In *Handbook of Physiology. Section I. The Nervous System.*, Mountcastle, V. B., Plum, F., and Geiger, S. R., Editors. 1987, American Physiological Society: Bethesda. p. 643-674.
3. Ogawa, S., Menon, R. S., Kim, S.-G., and Ugurbil, K., On the characteristics of functional magnetic resonance imaging of the brain. *Annual Review of Biophysics and Biomolecular Structure*, 1998. **27**: p. 447-474.
4. Motti, E., D. F., Imhof, H.-G., and Yasargil, M. G., The terminal vasculature bed in the superficial cortex of the rat: An SEM study of corrosion casts. *Journal of Neurosurgery*, 1986. **65**: p. 834-846.
5. Nakai, K., Imai, H., Kamei, I., Itakura, T., Komari, N., Kimura, H., Nagai, T., and Maeda, T., Microangioarchitecture of rat parietal cortex with special reference to vascular "sphincters": Scanning electron microscopic and dark field microscopic study. *Stroke*, 1981. **12**: p. 653-659.
6. Hughes, B. D., *Random Walks and Random Environments, Volume 2: Random Environments*. 1996, New York: Oxford Press.
7. Kleinfeld, D., Mitra, P. P., Helmchen, F., and Denk, W., Fluctuations and stimulus-induced changes in blood flow observed in individual capillaries in layers 2 through 4 of rat neocortex. *Proceedings of the National Academy of Sciences USA*, 1998. **95**: p. 15741-15746.
8. Tsai, P. S., Nishimura, N., Yoder, E. J., Dolnick, E. M., White, G. A., and Kleinfeld, D., Principles, design, and construction of a two photon laser scanning microscope for in vitro and in vivo brain imaging, In *In Vivo Optical Imaging of Brain Function*, Frostig, R. D., Editor. 2001, CRC Press.
9. Kleinfeld, D. and Denk, W., Two-photon imaging of neocortical microcirculation, In *Imaging Neurons: A Laboratory Manual*, Yuste, R., Lanni, F., and Konnerth, A., Editors. 2000, Cold Spring Harbor Laboratory Press: Cold Spring Harbor. p. 23.1-23.15.
10. Patel, U., Non-random distribution of blood vessels in the posterior region of the rat somatosensory cortex. *Brain Research*, 1983. **289**: p. 65-70.
11. Dirnagl, U., Villringer, A., and Einhaupl, K. M., *In-vivo* confocal scanning laser microscopy of the cerebral microcirculation. *Journal of Microscopy*, 1992. **165**: p. 147-157.
12. Carvell, G. E. and Simons, D. J., Biometric analyses of vibrissal tactile discrimination in the rat. *Journal of Neuroscience*, 1990. **10**: p. 2638-2648.

13. Ngai, A. C., Meno, J. R., and Winn, H. R., Simultaneous measurements of pial arteriolar diameter and laser-doppler flow during somatosensory stimulation. *Journal of Cerebral Blood Flow and Metabolism*, 1995. **15**: p. 124-127.
14. Biswal, B. B. and Hudetz, A. G., Synchronous oscillations in cerebrocortical capillary red blood flow after nitric oxide synthase inhibition. *Microvascular Research*, 1996. **52**: p. 1-12.
15. Golanov, E. V., Yamamoto, S., and Reis, D. J., Spontaneous waves of cerebral blood flow associated with a pattern of electrocortical activity. *The American Journal of Physiological*, 1994. **266**: p. R204-R214.
16. Mayhew, J. E. W., Askew, S., Zeng, Y., Porrill, J., Westby, G. W. M., Redgrave, P., Rector, D. M., and Harper, R. M., Cerebral vasomotion: 0.1 Hz oscillation in reflectance imaging of neural activity. *Neuroimage*, 1996. **4**: p. 183-193.
17. Mitra, P. P., Pesaran, B., Ogawa, S., Kleinfeld, D., and Ugerbil, K. Characterization and removal of respiratory, cardiac and vasomotor oscillations in dynamic brain images. In *Society for Neuroscience Annual Meeting*. 1995. San Diego, CA.
18. Tomita, M., Gotoh, F., Sato, T., Tanahashi, N., and Tanaka, K. 4-6 cycle per minute fluctuation in cerebral blood volume of feline cortical tissue in situ. *Journal of Cerebral Blood Flow and Metabolism (abstract)*, 1981. **1**: S443-S444.
19. Colantuoni, A., Bertuglia, S., and Intaglietta, M., Microvascular vasomotion: Origin of laser Doppler flux motion. *International Journal of Microcirculation*, 1994. **14**: p. 151-158.
20. Mitra, P. P., Ogawa, S., Hu, X., and Ugurbil, K., The nature of spatiotemporal changes in cerebral hemodynamics as manifested in functional magnetic resonance imaging. *Magnetic Resonance in Medicine*, 1997. **37**: p. 511-518.
21. Malonek, D., Dirnagl, U., Lindauer, U., Yamada, K., Kanno, I., and Grinvald, A., Vascular imprints of neuronal activity: Relationships between the dynamics of cortical blood flow, oxygenation, and volume changes following sensory stimulation. *Proceedings of the National Academy of Sciences, USA*, 1997. **94**: p. 14826-14831.
22. Thomson, D. J., Spectral estimation and harmonic analysis. *Proceedings of the IEEE*, 1982. **70**: p. 1055-1096.

Figure 1. Reconstruction of the capillary bed in rat cortex. The vasculature was filled with a casting material. After curing, the soft tissue was removed by corrosion in KOH and the casting was coated with gold and observed in the scanning electron microscope (SEM). The image on the left is the SEM data and the image on the right is the interpretation of the SEM image, with arterioles drawn in black, venules drawn in white, and capillaries shaded as gray. Note the closed loops and “T” junctions in the capillary bed. Data extracted from figure 9 in the work of Motti, Imhof and Yasargh [4].

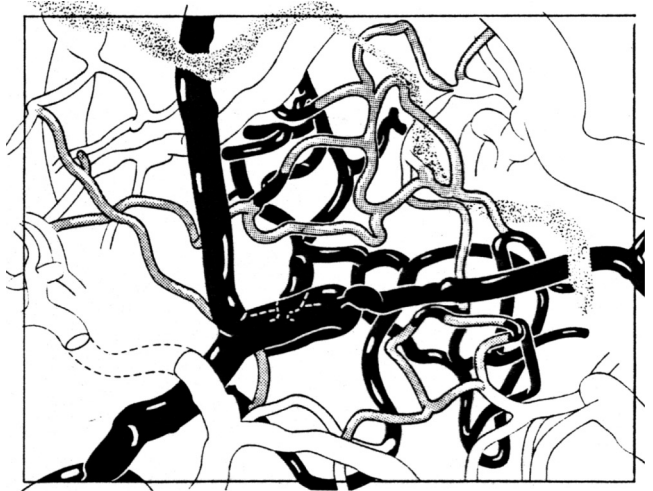
Figure 2. Characterization of individual capillaries and flow in the capillaries. **(a)** Tangential projection in the vicinity of a single capillary that is reconstructed from a set of 100 planar scans acquired every 1 μm between 310 and 410 μm . **(b)** The intensity profile along the cross-section for the scan that passed through the central axis of the capillary in question ($z = 360 \mu\text{m}$). The caliber is defined by the number of pixels whose intensity is above the background level, as noted. **(c)** Successive planar images through a small vessel, acquired every 60 ms. The change in position of a particular unstained object, interpreted as a RBC, is indicated by the series of arrows (\rightarrow); the velocity of the RBC is +0.18 mm/s. Depth = 450 μm . **(d)** Succession of line-scans (2 ms/line) through the axis of a capillary, shown solely to illustrate the characterization of RBC flow.

Figure 3. Characterization of the basal motion of RBCs in capillaries. The vessels were scanned at 2 ms/line, except for one vessel with very fast flow that was scanned at 1 ms/line. **(a - c)** Selected 1 s segments of the line-scan data for flow in three different vessels. Note the increase in speed and flux in the progression (a) \rightarrow (b) \rightarrow (c). **(d)** Representative plot of the spectral power in a 128 s record of speed versus time; we used multi-taper estimation techniques [22] with a half-bandwidth of 0.02 Hz. Note the peak near 0.1 Hz (*); the peak at 3.2 Hz is the aliased heart rate of 6.8 Hz. **(e)** Plot of the speed versus flux for flow in 38 vessels. The solid line is a best fit to points in the data set. **(h)** A 1 s segment of the line-scan data through a straight section of capillary in which the speed changes from relatively slow (large slope) to fast (small slope). **(i)** A 1 s segment of data at the onset of a transient stall in flow (S). Note that the RBCs remain stuck in the vessel. **(j)** A 1 s segment of data that shows the flow in two collinear arms of a junction. Note the reversal in the direction of flow in the arm on the left (R).

Figure 4. The nature of the single-trial response of red blood cell flow to vibrissa stimulation in a capillary in vibrissa primary S1 cortex. **(a)** A complete 128 s time-series with 6 separate stimuli,

spaced 20 s apart. Shown are the speed, the flux, and the ECoG recorded from a site 2 mm lateral to the optical measurement. Depth = 255 μm . **(b)** Trial-average of the quantities shown in part (a). The dark line is the average over all 6 trials, the gray band is the standard deviation of the trial average, and the thin straight line is drawn through the prestimulus portion of the data. **(c)** Spectral power for the speed shown in part (a) (thick line) along with the power for a record taken immediately after that in part (a) but in the absence of simulation (thin line). The '◆' corresponds to variation in the speed at the 0.05 Hz repetition frequency of the stimulation and the '*' corresponds to a peak at 0.1 Hz associated with vasomotor oscillations. The half-bandwidth of the spectral estimation was 0.016 Hz.

Figure 5. The single-trial time series of the speed of red blood cell flow during an epoch that includes mild electrical shock to the tail (1 s train of 3 ms pulses delivered at 20 Hz). The oscillations in the speed corresponds to 6.5 Hz modulation from cardiac pulsations. Note that the increase in flow in response to simulation peaks at 65 % above the basal level, as opposed to the much smaller change seen in response to natural vibrissa stimulation (Fig. 4a).



— 100 μm

